

Biocatalysis

International Edition: DOI: 10.1002/anie.201604014

German Edition: DOI: 10.1002/ange.201604014

Accelerating Enzymatic Catalysis Using Vortex Fluidics

Joshua Britton, Luz M. Meneghini, Colin L. Raston,* and Gregory A. Weiss*

Abstract: Enzymes catalyze chemical transformations with outstanding stereo- and regio-specificities, but many enzymes are limited by their long reaction times. A general method to accelerate enzymes using pressure waves contained within thin films is described. Each enzyme responds best to specific frequencies of pressure waves, and an acceleration landscape for each protein is reported. A vortex fluidic device introduces pressure waves that drive increased rate constants (k_{cat}) and enzymatic efficiency (k_{cat}/K_m). Four enzymes displayed an average seven-fold acceleration, with deoxyribose-5-phosphate aldolase (DERA) achieving an average 15-fold enhancement using this approach. In solving a common problem in enzyme catalysis, a powerful, generalizable tool for enzyme acceleration has been uncovered. This research provides new insights into previously uncontrolled factors affecting enzyme function.

Enzymes make life possible by catalyzing diverse and challenging chemical transformations with exquisite specificity. Applications in both industry^[1] and academia^[2] rely on the selectivity and power of enzymes to catalyze otherwise challenging transformations. Biocatalysts offer remarkable rate accelerations compared to the uncatalyzed reactions, with typical rate accelerations (k_{cat}/k_{uncat}) of 10^5 - to 10^{15} -fold faster.^[3] Though some enzymes are diffusion-limited,^[4] the catalytic rates of enzymes are more typically limited by their catalytic efficiency (k_{cat}/K_m); additionally, molecular crowding, along with product and substrate inhibition, can reduce enzyme efficiency.^[5] Though some enzymes catalyze transformations with rapid rates (for example, laccases, fumarases, and alcohol dehydrogenases),^[6] other enzymes operate at only modest reaction rates, requiring long reaction times and carefully optimized conditions; for example, DERA requires long processing times (hours to days), and is substrate-inhibited.^[7] We report a process that accelerates four different enzymes at standard temperature and pressure, but many other water-soluble enzymes could be accelerated as well.

Recently, vortex fluidic devices (VFDs) have been used to accelerate covalent and noncovalent bond formation. VFDs

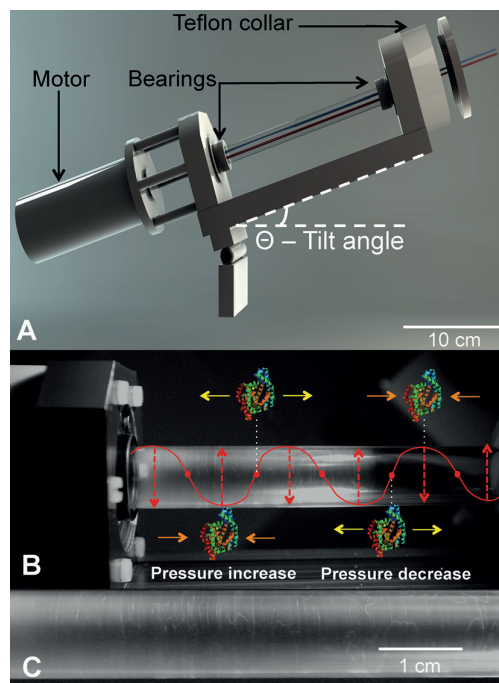


Figure 1. The VFD and its Faraday waves. A) A representation of the VFD. B) A VFD sample tube, containing 5 mL of solution rotating at 3500 rpm at a tilt angle θ of 45° , shows Faraday waves formed within the thin film. Such pressure waves, shown as an overlaid representation, can affect the enzyme–substrate complex. C) Enlargement of the VFD-generated Faraday waves. Additional images of the Faraday waves can be found in the Supporting Information, Figure S14.

process solutions in thin films by the rapid rotation of a sample tube (Figure 1).^[8] Within the thin film, species are subjected to high levels of shear stress, mass transfer, and vibrational energy input at specific rotational speeds. For example, the VFD demonstrated the effective folding of four different proteins within minutes at standard temperature and pressure.^[9] The VFD has also been used to improve the synthesis of lidocaine^[10] and several other organic transformations.^[11] In a continuous flow regime, flow rates of up to 20 mL min^{-1} can be achieved to process up to 30 L per day in the current benchtop configuration. Since VFD processing increased the rates of organic reactions and protein folding, we hypothesized that biocatalysis, which requires both reactivity and the correct protein fold, could benefit as well.

Control reactions with alkaline phosphatase demonstrated the requirements for high, specific rotational speeds of the VFD to generate a thin film containing the enzyme for accelerated catalysis (Supporting Information, Figures S2–4). VFD-mediated acceleration of four biocatalysts was com-

[*] J. Britton, Prof. Dr. C. L. Raston
Chemical and Physical Sciences, Flinders University
Bedford Park, Adelaide, 5001 (Australia)
E-mail: Colin.Raston@flinders.edu.au

J. Britton, Prof. Dr. G. A. Weiss
Department of Chemistry, University of California, Irvine
Irvine, CA 92697-2025 (USA)
E-mail: Gweiss@uci.edu

L. M. Meneghini, Prof. Dr. G. A. Weiss
Department of Molecular Biology and Biochemistry
University of California, Irvine
Irvine, CA 92697-2025 (USA)

Supporting information for this article can be found under:
<http://dx.doi.org/10.1002/anie.201604014>.

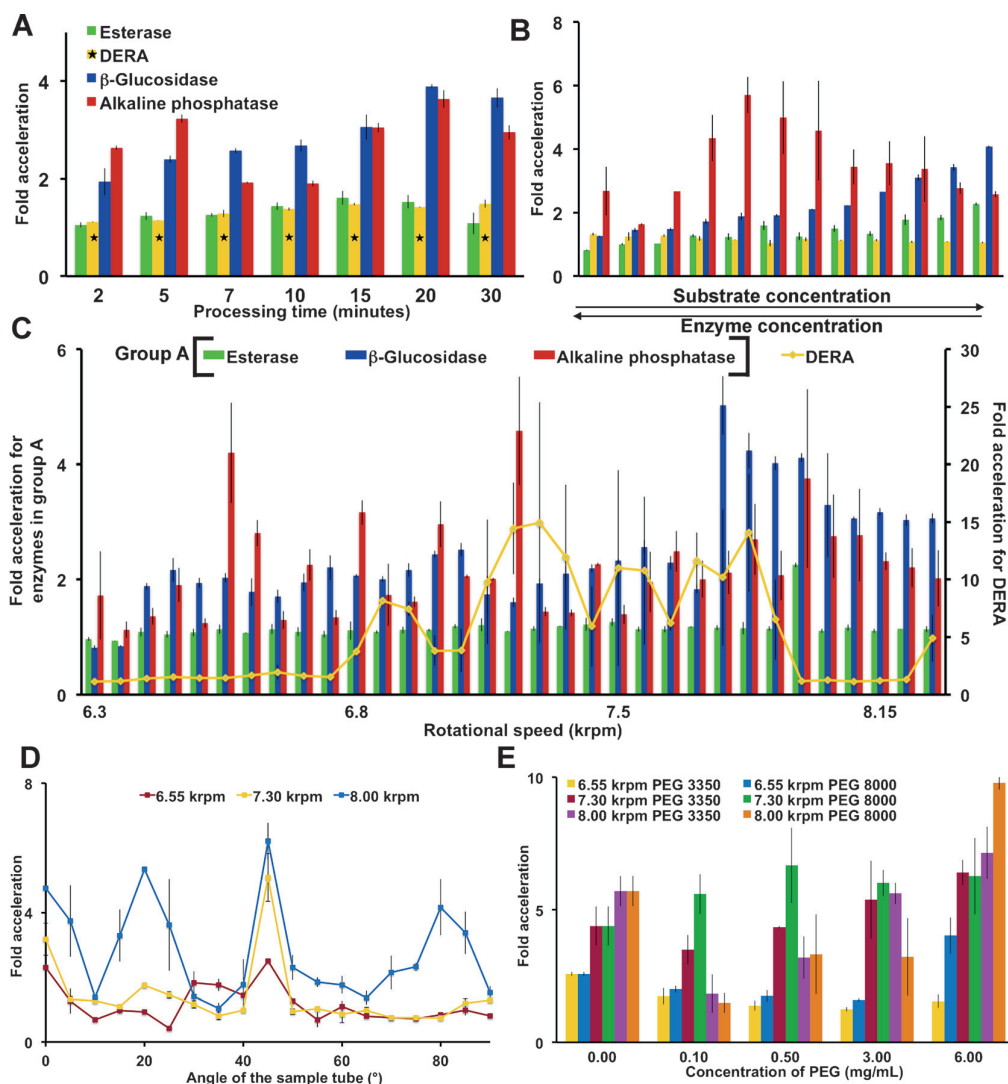


Figure 2. Parameters for accelerated biocatalysis of the four enzymes. Fold acceleration was determined as the ratio of the VFD-mediated substrate conversion to that of an identical enzyme–substrate solution not treated with the VFD. A) A time dependent study at a fixed rotational speed (8000 rpm) reveals processing times for further optimization. As indicated with a *, DERA required longer reaction times of 60, 80, 100, 120, 140, 160, and 180 min. B) Simultaneous changes to the substrate and enzyme concentrations at a 8000 rpm rotational speed mapped the reaction landscape (Supporting Information, Table S2A–D). C) Rotational speed scans in 50 rpm increments identify harmonic oscillations associated with Faraday wave-promoted biocatalysis. Error bars are larger for DERA than for any other enzyme due to the non-linear fluorescence calibration curve of the product. D) Varying the tilt angle of the sample tube when processing alkaline phosphatase and its substrate identified 45° as the optimal angle. Thus, a 45° tilt angle was used herein. E) The addition of PEG dramatically affects alkaline phosphatase catalysis in the non-VFD control. However, the VFD-processed solution demonstrated significant catalytic activity. Error bars indicate the standard deviation around the mean ($n=3$ with three independent measurements on three different VFDs). With the exception of a single data point requiring 90% confidence limits, all data reported have no overlapping errors within 95% confidence limits. The concentrations of the enzymes and substrates are as follows: fast alkaline phosphatase (6.77 nM) and its substrate *p*-nitrophenol phosphate (0.17 mM), β -glucosidase (19.3 nM) and its substrate 4-nitrophenyl β -D-glucopyranoside (7.5 mM), esterase (0.12 nM) and its substrate *p*-nitrophenol acetate (44 μ M), and DERA (7.69 μ M) and its fluorogenic substrate (0.52 mM) unless otherwise indicated, and as described in the Supporting Information, Table S2A–D.

pared to identical unprocessed enzyme–substrate solutions for efficient reaction optimization (Figure 2). The VFD processing times were varied to identify short time periods (2 min to 3 h) suitable for further optimization (Figure 2A). Esterase produced a lower VFD-based enhancement (two-fold) compared to the other three enzymes; esterase also needed longer reaction times due to the enzyme's requirements for low

substrate concentrations.^[12] In general, after long time periods, the substrate is expended and the unprocessed solution can reach similar levels of substrate conversion. Furthermore, the VFD-processed solutions have parallel activities to their non-VFD counterparts for the first few minutes before the rapid acceleration of the former (for example, alkaline phosphatase in the Supporting Information,

Figure S9). A similar lag period before rate acceleration has been described previously for ultrasound-accelerated enzyme acceleration.^[13]

The substrate and enzyme concentrations were simultaneously varied for the rapid scanning of reaction space to find effective reaction conditions (Figure 2B). This optimization unexpectedly revealed that VFD-mediated enzyme reactions are less susceptible to substrate inhibition than the conventional conditions. For example, β -glucosidase without VFD processing encounters substrate inhibition at around 3.1 mM 4-nitrophenyl β -D-glucopyranoside; VFD processing prevents the onset of substrate inhibition up to an almost three-fold higher concentration (Supporting Information, Figure S10B). With the exception of DERA, the three other enzymes tolerated higher concentrations of substrate without losing VFD-mediated acceleration. This decrease in substrate inhibition suggests that the VFD increases the enzymatic k_{cat} , as further demonstrated below. DERA catalyzed the retro-aldol reaction of a pro-fluorophore at $144 \mu\text{mol h}^{-1} \text{L}^{-1}$ when processed in the VFD (7900 rpm rotational speed), compared to $10.7 \mu\text{mol h}^{-1} \text{L}^{-1}$ under non-VFD conditions. DERA has previously been employed to synthesize high-value, complex, polyoxygenated compounds.^[7b] The VFD-mediated DERA reaction achieved an average 15-fold enhancement. Conventional approaches to improving DERA have applied extensive screening^[7b] and multiple rounds of error-prone PCR. For example, screening 20 000 colonies yielded a 10-fold increase in DERA activity.^[14] The efforts required to achieve a greater than 10-fold acceleration by the VFD in several days compared with conventional protein engineering, highlight the power of the approach reported here.

Enzyme acceleration by the VFD is sensitive to the tilt angle of the sample tube and the viscosity of the solution (Figure 2D,E). A tilt angle of 45° produced the strongest response, as has been previously observed in other VFD experiments.^[8b] Furthermore, high concentrations of viscous, steric-crowding reagents that decrease or terminate enzymatic catalysis in the non VFD-mediated control conditions were overcome in the VFD. Biocatalytic acceleration was achieved, for example, in high concentrations of PEG 8000 (6.00 mg mL^{-1} , 0.75 M), a condition that suppresses enzymatic catalysis in non-VFD-mediated reactions. Through rapid micro mixing or other associated phenomena, VFD-processed alkaline phosphatase tolerated high concentration of PEG 8000, resulting in a circa 9-fold enhancement. The relative indifference to high concen-

trations of substrate and steric crowding suggests that the VFD could be applied to processes requiring complex mixtures and minimal amounts of solvent.

The dependence on rotational speeds was also specific to each enzyme (Figure 2C and the Supporting Information, Figure S11). Such requirements likely reflect differences in enzyme size, structure, and dynamics. Esterase, for example, was highly dependent on a single rotational speed for enhanced activity. When processing esterase under VFD-mediated conditions, the only rotational speed to generate an enhancement was 8000 rpm; at all other rotational speeds, the enzyme behaved similarly to the non-VFD-mediated conditions. To map out the fine details of such resonances, a high-resolution scan of rotational speeds examined the acceleration of alkaline phosphatase and β -glucosidase (Figure 3). The rotational landscapes are intricate with little overlap of the optimal rotational speeds for each enzyme. Device-specific variations in rotational landscapes were also observed, likely due to differences between device bearings and components (for example, the Teflon collar, which wears out due to friction from the sample tube); thus, Figure 3 depicts two enzymes processed by a single VFD. In addressing this issue of wear, and avoiding variable vibrations, we turned to 3D printing. Fabricating the collar out of high-density ABS plastic allowed an interchangeable sleeve to be incorporated. Changing the insert upon wear insures reproducibility of the reported experiments (Supporting Information, Figure S19).

Michaelis–Menten-based experiments were performed with β -glucosidase, and the kinetic constants derived for both the VFD- and non-VFD processed solutions (Table 1). The k_{cat} in the VFD-mediated reaction was around 2.5-fold faster than the non-VFD reaction (Figure 3 and Table 1). A lower Michaelis–Menten constant (K_{m}) was also obtained for the VFD-processed enzyme–substrate solution; 2.50 mM compared to 3.76 mM for a non-VFD-mediated reaction. The decrease in K_{m} demonstrates the higher affinity for the β -

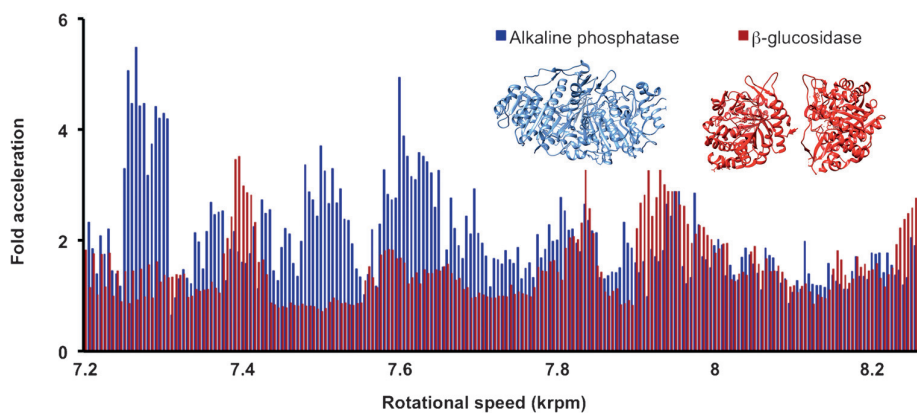


Figure 3. The rotational landscape of β -glucosidase and alkaline phosphatase. Though the two enzymes have similar levels of response at some rotational speeds, distinctly different rotational landscapes are revealed. The results demonstrate the enzyme specificity of VFD-mediated acceleration. Each data point represents the mean ($n=2$) for a 10 min reaction at the indicated rotational speed. The alkaline phosphatase enzyme–substrate solution used fast alkaline phosphatase (6.77 nM) and *p*-nitrophenol phosphate solution (0.17 mM) whilst the β -glucosidase enzyme–substrate system used β -glucosidase (19.3 nM) and 4-nitrophenyl β -D-glucopyranoside (7.5 mM).

Table 1: Michaelis–Menten parameters for the VFD versus non-VFD-mediated processing of β -glucosidase.^[a]

Parameter	Non VFD-mediated reaction	VFD-mediated rate acceleration
V_{\max} [nM s ⁻¹]	128 ± 5.71	309 ± 52.4
K_m [mM]	3.76 ± 0.15	2.50 ± 0.44
k_{cat} [s ⁻¹]	13.4 ± 0.59	32.1 ± 5.45
k_{cat}/K_m [mM ⁻¹ s ⁻¹]	3.55 ± 0.19	13.32 ± 4.03

[a] For the VFD process with β -glucosidase (9.26 nM), a rotational speed of 7600 rpm was used, as this provided the most consistent enhancement over sustained time periods. Errors indicate the standard deviation around the mean ($n=3$). There was no overlapping error at 95% confidence limits. The raw data was fitted to the Michaelis–Menten equation using a least squares fitting (LSF) approach (Supporting Information, Figures S17 and S18 and Table S3).

glucosidase–substrate interaction under VFD-mediated conditions. The increase of k_{cat} and the decrease in K_m leads to an approximately 3.5-fold increase in enzyme efficiency (k_{cat}/K_m) for the VFD-mediated reaction.

We hypothesize that enzymes are accelerated in the VFD by the instantaneous pressure changes generated by Faraday waves. Three possible mechanisms could harness such pressures. First, transient pressurization of the active site around the substrate could occur. In this situation, a decrease in the active site volume through pressurization^[15] could increase the turnover number of the enzyme; such enhancement follows from the Van't Hoff equation.^[16] Second, beneficial pressure-induced protein conformational changes could occur at accelerated rates.^[17] As enzymatic catalysis correlates with protein motion, faster enzyme oscillations could accelerate catalysis by contributing to the rate-determining process.^[17] Third, enzymatic catalysis requires a fine balance between protein stability and conformational flexibility.^[18] Pressure-driven conformational changes may increase enzyme activity through β - and α -relaxations.^[19] These small changes can lead to the acquisition of protein conformations more suited for catalysis.^[18]

The rotational landscape is specific for each enzyme studied and appears to result from enzyme-specific preferences. Single-molecule experiments have elucidated the range of speeds and conformations required for enzymatic catalysis, which are specific for each enzyme.^[20] The range of acceleration observed here falls within the expected range of enzyme speeds uncovered through such experiments. Thus, the VFD-driven rate acceleration could simply shift the distribution of enzyme conformational states to favor catalytic events. In future experiments, shaped Faraday waves with specific timing could provide further control and enhancement of biocatalysis.

In conclusion, we have demonstrated that the VFD effectively accelerates four enzymes and established a general, simple method to make biocatalysis more practical. VFD-mediated rate acceleration could find broad applicability in chemical transformations at industrial and laboratory scales.

Acknowledgements

J.B. thanks the Taihi Hong Memorial Foundation and Kritika Mohan for photography. L.M.M. acknowledges the Miguel Velez Scholarship at UCI. G.A.W. gratefully acknowledges the National Institute of General Medical Sciences of the NIH (RO1-GM100700-01). C.L.R. acknowledges the Australian Research Council and the Government of South Australia for their financial support during this project.

Keywords: aldolases · biocatalysis · enzyme acceleration · hydrolases · vortex fluidics

How to cite: *Angew. Chem. Int. Ed.* **2016**, *55*, 11387–11391
Angew. Chem. **2016**, *128*, 11559–11563

- [1] a) W. Aehle, *Enzymes in Industry*, Wiley-VCH, Weinheim, **2004**; b) B. M. Nestl, B. A. Nebel, B. Hauer, *Curr. Opin. Chem. Biol.* **2011**, *15*, 187–193; c) R. DiCosimo, J. McAuliffe, A. J. Poulou, G. Bohlmann, *Chem. Soc. Rev.* **2013**, *42*, 6437–6474; d) D. J. Pollard, J. M. Woodley, *Trends Biotechnol.* **2007**, *25*, 66–73; e) J.-M. Choi, S.-S. Han, H.-S. Kim, *Biotechnol. Adv.* **2015**, *33*, 1443–1454.
- [2] a) H. Renata, Z. J. Wang, F. H. Arnold, *Angew. Chem. Int. Ed.* **2015**, *54*, 3351–3367; *Angew. Chem.* **2015**, *127*, 3408–3426; b) Z. J. Wang, H. Renata, N. E. Peck, C. C. Farwell, P. S. Coelho, F. H. Arnold, *Angew. Chem. Int. Ed.* **2014**, *53*, 6810–6813; *Angew. Chem.* **2014**, *126*, 6928–6931; c) J. B. Siegel, A. L. Smith, S. Poust, A. J. Wargacki, A. Bar-Even, C. Louw, B. W. Shen, C. B. Eiben, H. M. Tran, E. Noor, J. L. Gallaher, J. Bale, Y. Yoshikuni, M. H. Gelb, J. D. Keasling, B. L. Stoddard, M. E. Lidstrom, D. Baker, *Proc. Natl. Acad. Sci. USA* **2015**, *112*, 3704–3709; d) S. Wallace, E. P. Balskus, *Angew. Chem. Int. Ed.* **2015**, *54*, 7106–7109; *Angew. Chem.* **2015**, *127*, 7212–7215; e) P. Srivastava, H. Yang, K. Ellis-Guardiola, J. C. Lewis, *Nat. Commun.* **2015**, *6*, 7789.
- [3] a) A. S. Bommaris, B. R. Riebel, *Biocatalysis*, Wiley-VCH, Weinheim, **2004**; b) K. M. Koeller, C.-H. Wong, *Nature* **2001**, *409*, 232–240; c) V. L. Schramm, *Annu. Rev. Biochem.* **1998**, *67*, 693–720.
- [4] M. E. Stroppolo, M. Falconi, A. M. Caccuri, A. Desideri, *CMLS Cell. Mol. Life Sci.* **2001**, *58*, 1451–1460.
- [5] D. L. Nelson, M. M. Cox, *Lehninger Principles of Biochemistry*, 5th ed., W. H. Freeman, New York, **2008**.
- [6] R. Wolfenden, M. J. Snider, *Acc. Chem. Res.* **2001**, *34*, 938–945.
- [7] a) F. Subrizi, M. Crucianelli, V. Grossi, M. Passacantando, G. Botta, R. Antiochia, R. Saladino, *ACS Catal.* **2014**, *4*, 3059–3068; b) W. A. Greenberg, A. Varvak, S. R. Hanson, K. Wong, H. Huang, P. Chen, M. J. Burk, *Proc. Natl. Acad. Sci. USA* **2004**, *101*, 5788–5793.
- [8] a) J. Britton, S. B. Dalziel, C. L. Raston, *Green Chem.* **2016**, *18*, 2193–2200; b) J. Britton, S. B. Dalziel, C. L. Raston, *RSC Adv.* **2015**, *5*, 1655–1660.
- [9] T. Z. Yuan, C. F. G. Ormonde, S. T. Kudlacek, S. Kunche, J. N. Smith, W. A. Brown, K. M. Pugliese, T. J. Olsen, M. Iftikhar, C. L. Raston, G. A. Weiss, *ChemBioChem* **2015**, *16*, 393–396.
- [10] J. Britton, J. M. Chalker, C. L. Raston, *Chem. Eur. J.* **2015**, *21*, 10660–10665.
- [11] a) L. Yasmin, X. Chen, K. A. Stubbs, C. L. Raston, *Sci. Rep.* **2013**, *3*, 2282; b) J. Britton, C. L. Raston, *RSC Adv.* **2014**, *4*, 49850–49854; c) J. Britton, C. L. Raston, *RSC Adv.* **2015**, *5*, 2276–2280.
- [12] F. M. Menger, M. Ladika, *J. Am. Chem. Soc.* **1987**, *109*, 3145–3146.

- [13] K. Zhu, H. Liu, P. Han, P. Wei, *Front. Chem. Eng. China* **2010**, *4*, 367–371.
- [14] S. Jennewein, M. Schürmann, M. Wolberg, I. Hilker, R. Luiten, M. Wubbolts, D. Mink, *Biotechnol. J.* **2006**, *1*, 537–548.
- [15] N. Hillson, J. N. Onuchic, A. E. García, *Proc. Natl. Acad. Sci. USA* **1999**, *96*, 14848–14853.
- [16] C. J. T. Kuster, H. W. Scheeren, *In High Pressure Chemistry*, Wiley-VCH, Weinheim **2007**.
- [17] S. Hay, N. S. Scrutton, *Nat. Chem.* **2012**, *4*, 161–168.
- [18] K. A. Henzler-Wildman, M. Lei, V. Thai, S. J. Kerns, M. Karplus, D. Kern, *Nature* **2007**, *450*, 913–916.
- [19] U. R. Shrestha, D. Bhowmik, J. R. D. Copley, M. Tyagi, J. B. Leão, X.-q. Chu, *Proc. Natl. Acad. Sci. USA* **2015**, *112*, 13886–13891.
- [20] a) P. C. Sims, I. S. Moody, Y. Choi, C. Dong, M. Iftikhar, B. L. Corso, O. T. Gul, P. G. Collins, G. A. Weiss, *J. Am. Chem. Soc.* **2013**, *135*, 7861–7868; b) S. Xie, *Single Mol.* **2001**, *2*, 229–236.

Received: April 25, 2016

Published online: August 5, 2016